

Radial distribution of magnetic permeability in amorphous CoFeNbSiB wires

© A.A. Moiseev, D.A. Bukreev, M.S. Derevyanko, A.V. Semirov

Irkutsk State University,
664003 Irkutsk, Russia
e-mail: Moiseev.AI.An@gmail.com

Received July 23, 2023

Revised October 24, 2023

Accepted November 10, 2023

The paper presents the results of the estimation of the radial distribution of magnetic permeability in amorphous $\text{Co}_{66}\text{Fe}_4\text{Nb}_{2.5}\text{Si}_{12.5}\text{B}_{15}$ wires by magnetoimpedance tomography. It was found that the radial distribution of the magnetic permeability is significantly non-uniform. In this case, the magnetic permeability takes a minimum value close to unity near the wire axis, and maximum values of several thousand in the middle part of the wire cross-section. It is shown that the magnetic permeability is largely determined by the magnitude and ratio of internal quenching stresses components in the deep regions of the wire. In the surface region of the wire, the value of the magnetic permeability can be significantly influenced by demagnetizing fields arising from inhomogeneities in the surface relief.

Keywords: magnetoimpedance tomography, magnetic impedance effect, finite element method, computer modeling, amorphous wires.

DOI: 10.61011/JTF.2024.01.56903.189-23

Introduction

The technology of production of metal alloys in an amorphous state involves rapid quenching from a melt. Amorphous metal alloys are in a stressed state as a result of this operation, which is characterized by a significant amount of internal mechanical stresses and their inhomogeneous distribution in the volume of the alloy [1,2]. The radial distribution of quenching stresses deserves the main attention if the alloys are obtained in the form of wires of cylindrical geometry. This distribution can be estimated based on the consideration of the melt solidification process [3,4], or based on the consideration of the radial distribution of material properties that exhibit dependence on quenching stresses. Both approaches do not provide a clear answer and have a number of significant assumptions. However, they can be used complementing each other.

Amorphous alloys based on transition metals have strongly pronounced magnetic properties. These materials are already used in various practical applications because of the significant magnitude of the magnetic permeability, as well as its sensitivity to various external impacts [5,6]. On the other hand, it is the magnetic permeability of amorphous ferromagnets that is one of the indicators that allows analyzing the processes occurring in them.

As noted above, the radial distribution of quenching stresses is of particular interest in case of amorphous ferromagnetic alloys produced in the form of cylindrical geometry wires. The world scientific community believes that magnetic anisotropy has a magnetoelastic nature in this class of materials [3,4]. The magnetic anisotropy constant is determined by the effective value of quenching

stresses according to these concepts and the direction of the anisotropy axis depends on the ratio of the components of these stresses and the sign of the magnetostriction constant. The parameters of magnetic anisotropy affect the magnitude of magnetic permeability and the nature of its change under various external impacts. The behavior of the circular magnetic permeability μ in an amorphous cylindrical conductor exposed to an axial magnetic field can be described as follows [7]:

- the maximum value of μ is achieved in the absence of an external axial magnetic field, therefore, magnetic anisotropy prevails the axial component;
- the maximum value of μ is reached at a certain value of the external axial magnetic field, therefore, the circular component prevails in magnetic anisotropy.

Therefore, the magnetic field dependence of the magnetic permeability makes it possible to evaluate the properties of magnetic anisotropy. Several methods can be used for experimental determination of the magnetic field dependence of the magnetic permeability. For example, an analysis of the hysteresis properties of the studied samples provides the understanding of the magnetic field dependence of the effective magnetic permeability of the entire sample volume. In turn, the analysis of the behavior of high-frequency electrical impedance in an external magnetic field due to the skin effect makes it possible to evaluate the magnetic field dependence of the circular magnetic permeability of individual layers of the sample. This method of magnetoimpedance tomography (MIT) is based on the said capability. The principle of the MIT is to select such numerical values of the electromagnetic and geometric parameters of the model of the studied sample,

which ensure a good conformance of the experimental and calculated dependences of the electrical impedance on the alternating current frequency [8].

This paper discusses the possibility of estimation of the radial distribution of the circular magnetic permeability of cylindrical conductors obtained by rapid quenching of a ferromagnetic alloy using the MIT method, as well as physical factors resulting in a non-monotonic dependence of the circular magnetic permeability on the radial coordinate.

1. Modeling, samples and experimental techniques

The studied samples were represented by a model of n coaxial cylindrical regions (layers) for implementation of the MIT method. Magnetic permeability μ_i , electrical conductivity γ_i and external radius r_i were set for each wire layer. The value r_n is equal to the radius of the wire. The conductivity γ was assumed to be the same in all parts of the wire. A model with $n = 5$ was considered, which is optimal in terms of information content and computational complexity. The models of the studied samples with $n = 2$ and 3 were considered by the authors earlier [8]. The finite element method was used for calculation of dependences of the given impedance on the alternating current frequency $Z(f)/R_{DC}$. The frequency of f was changed in the range from 0.01 to 100 MHz. Comsol Multiphysics software package was used for direct calculation (license № 9602434). It was ensured that the size of elements of the finite-element grid was less than the thickness of the skin layer when building the finite element grid. An array of simulated dependencies of $Z(f)/R_{DC}$ was obtained by varying the values of μ_i and r_i . Further, a dependence was found in this array that has the smallest absolute deviation from a similar dependence obtained experimentally.

The dependences of high-frequency electrical impedance on the alternating current frequency were experimentally studied using the segments of amorphous fast-quenched wire $\text{Co}_{66}\text{Fe}_4\text{Nb}_{2.5}\text{Si}_{12.5}\text{B}_{15}$ obtained by the fast quenching from the melt at the Bardin Central Research Institute for Ferrous Metallurgy with a radius of $r_n = 90 \mu\text{m}$ and a length of 90 mm. The active length of the sample through which the electric current flowed was 24 mm. All the studied samples were in their initial state. The magnetostriction constant is positive, about 10^{-7} . The results of the study of the magnetic and magnetoimpedance properties of these wires are presented in sufficient detail by the authors of this paper [9,10].

Magnetoimpedance spectroscopy measurement system was used for measurement of the electrical impedance module Z [11] in the AC frequency range, f , (0.01–100) MHz flowing along the length of the sample. The effective value of the current was 1 mA. An external magnetic field H was oriented along the length of the sample, the maximum strength of which was $H_{\max} = \pm 12.3 \text{ kA/m}$. The magnetoimpedance (MI) ratio was calculated for quantification of

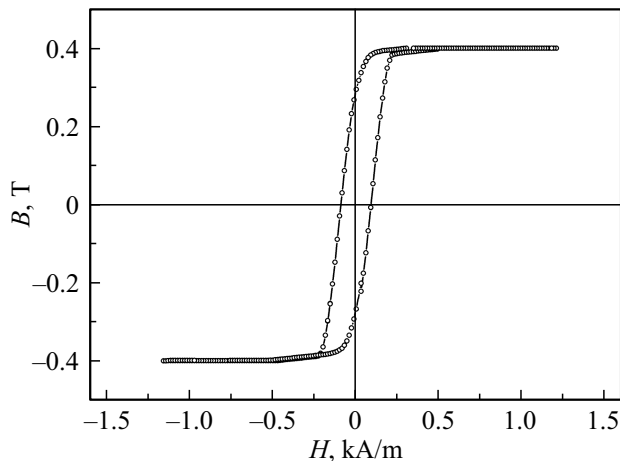


Figure 1. Longitudinal loop of magnetic hysteresis of amorphous wire $\text{Co}_{66}\text{Fe}_4\text{Nb}_{2.5}\text{Si}_{12.5}\text{B}_{15}$.

the dependence $Z(H)$:

$$\frac{\Delta Z}{Z}(H) = \frac{Z(H) - Z(H_{\max})}{Z(H_{\max})} 100\%.$$

2. Results and discussion

The magnetic hysteresis loops obtained by induction method with axial remagnetization reversal with a frequency of 1 kHz indicate a predominantly axial orientation of magnetization in the volume of the wire (Fig. 1).

Magnetic field dependences of the impedance obtained at different alternating current frequencies indicate a heterogeneity of the distribution of circular magnetic permeability in the cross section of the wire. Further, the circular magnetic permeability is covered. The MI and the nature of its magnetic field dependence also changes with an increase of the frequency of alternating current (Fig. 2).

The maximum MI is observed in the absence of an external magnetic field at alternating current frequencies of 2 MHz and below. The MI reaches its maximum value in magnetic fields with a strength of (40–190) A/m at AC frequencies above 2 MHz. Therefore, at least two regions with different magnetic permeability parameters can be defined in the cross section of the wire. However, MIT using a two-layer model prevents from reaching a good consistency between the simulated and experimental dependencies $Z(f)/R_{DC}$ [8]. The simulated dependence $Z(f)/R_{DC}$ can be significantly approximated to the experimental dependence by introducing a thin surface layer into the wire model to account for the effect of inhomogeneities of the surface of a real sample on magnetic permeability. However, this does not allow obtaining a good approximation in the low frequency region [8]. Taking into account the skin effect, it can be assumed that additional internal layers should be introduced into the model for approximating the simulated

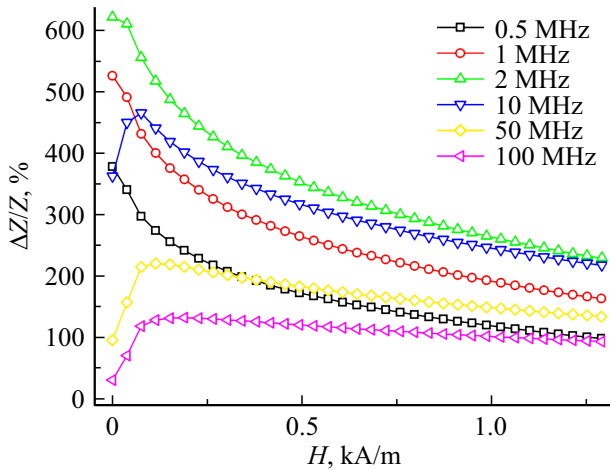


Figure 2. The dependences of the magnetoimpedance (MI) ratio on the external axial magnetic field, measured at different alternating current frequencies, on the state of technical saturation.

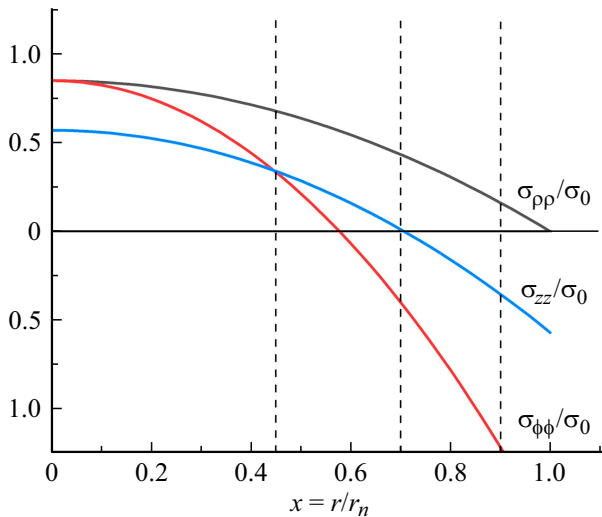


Figure 3. The radial distribution of the diagonal components of quenching stresses in an amorphous cylindrical wire produced by rapid quenching from a melt [4].

dependence $Z(f)/R_{DC}$ to the experimental dependence in the low frequency region.

The calculated dependencies of the quenching stress components were used for determination of the number of layers and an approximate estimate of their geometric position [4]. These calculated dependences were obtained for wires produced using a similar technology from an alloy that has a similar composition with the studied wires. The approximate relations describing the radial distribution of the diagonal components of quenching stresses in a cylindrical coordinate system can be represented as follows (Fig. 3): $\sigma_{\rho\rho}/\sigma_0 = 0.85 \cdot (1 - x^2)$; $\sigma_{\phi\phi}/\sigma_0 = 0.85 \cdot (1 - 3x^2)$; $\sigma_{zz}/\sigma_0 = 0.57 \cdot (1 - 2x^2)$, where $\sigma_{\rho\rho}$, $\sigma_{\phi\phi}$, σ_{zz} , σ_0 — diagonal (main) components

and amplitude of quenching stresses, $x = r/r_n$ — the equivalent radius.

Qualitatively, these dependencies can be divided into the following areas:

$0 - 0.45r_n$ — slight change of the diagonal (main) components of quenching stresses, while the values of these components are positive and their ratio is maintained $\sigma_{\rho\rho} \geq \sigma_{\phi\phi} \geq \sigma_{zz}$;

$0.45 - 0.7r_n$ — a sharp decrease of the modulus of the axial and circular components of quenching stresses, while the values of these components decrease to zero, and the circular component changes its sign;

$0.7 - 0.9r_n$ — an increase of the modulus of the axial and circular components of quenching stresses with negative values of these components, a sharp decrease of the positive radial component;

$0.9 - 1r_n$ — significant predominance of the negative circular component of quenching stresses, zero value of the radial component.

Varying the outer radii of the model regions within the designated boundaries allowed selecting their optimal values, namely $r_1 = 30 \mu\text{m}$ ($0.3r_n$); $r_2 = 60 \mu\text{m}$ ($0.67r_n$); $r_3 = 76 \mu\text{m}$ ($0.84r_n$); $r_4 = 88 \mu\text{m}$ ($0.98r_n$); $r_5 = 90 \mu\text{m}$. The best approximation of the simulated dependence $Z(f)/R_{DC}$ to the experimental dependence (Fig. 4, a), namely, the absolute deviation of not greater than 6% between them in the entire frequency range, including the low frequency range, is obtained with the following combination of electromagnetic parameters: $\gamma = 0.87 \text{ MCm/m}$; $\mu_1 = 1$; $\mu_2 = 11800$; $\mu_3 = 3400$; $\mu_4 = 6400$; $\mu_5 = 320$ (Fig. 4, b).

It should be noted that the magnetic permeability values were varied in the range from 1 to 1000 in increments of 10, and the magnetic permeability values of over 1000 were selected in increments of 50. Therefore, about 10^6 models with different combinations of electromagnetic and geometric parameters were constructed and analyzed for obtaining the discussed radial distribution of magnetic permeability.

The obtained numerical values of the magnetic permeability of the wire layers can be determined by the following physical factors:

— the minimum value of the magnetic permeability near the axis of the wire ($\mu_1 = 1$; $r_1 = 30 \mu\text{m}$) is probably attributable to the high value of the effective magnetic anisotropy constant of a magnetically elastic nature because of the significant quenching stresses in the axial region, and mainly the axial orientation of its axis, which is consistent with the magnetic loop hysteresis and magnetic field dependences of the impedance obtained in the low frequency range of alternating current;

— the maximum value of the magnetic permeability inside the wire ($\mu_2 = 11800$; $r_2 = 60 \mu\text{m}$) is probably attributable to a sharp decrease of the modulus of the axial and circular components of quenching stresses and, as a result, a significant decrease of the effective magnetic anisotropy constant;

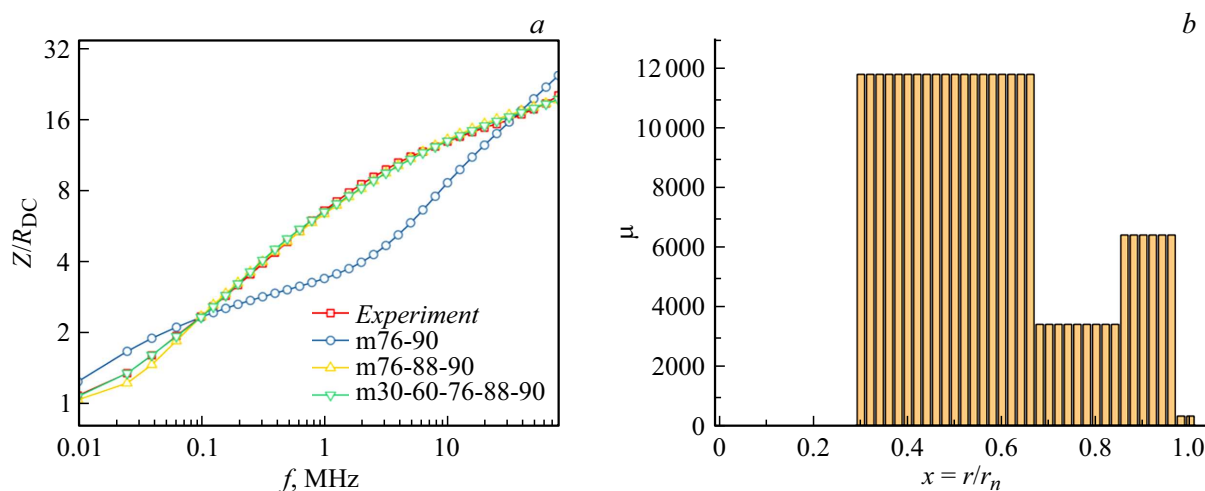


Figure 4. *a* — frequency dependences of the given impedance value, measured experimentally and obtained by the MIT method using different models (the model designation indicates the outer radii of the layers in micrometers), *b* — radial distribution of magnetic permeability in amorphous wires $\text{Co}_{66}\text{Fe}_4\text{Nb}_{2.5}\text{Si}_{12.5}\text{B}_{15}$ in the absence of an external magnetic field.

— high values of magnetic permeability near the surface of the wire ($\mu_3 = 3400$; $\mu_4 = 6400$; $r_3 = 76\ \mu\text{m}$; $r_4 = 88\ \mu\text{m}$) are probably attributable to a low value of the effective magnetic anisotropy constant;

— the low value of the magnetic permeability on the surface of the wire ($\mu_5 = 320$; $r_5 = 90\ \mu\text{m}$) is probably attributable to the additional impact of demagnetizing fields occurring from the surface morphology features of the studied samples.

Conclusion

Therefore, it was shown that the radial distribution of the circular magnetic permeability in amorphous cylindrical cobalt-based conductors obtained by rapid quenching from a melt can be estimated by the MIT method. The non-monotonic dependence of the magnetic permeability on the radial coordinate is facilitated by the complex distribution of internal quenching stresses due to the method of production. It is assumed that the magnetoelastic mechanism is not the only one in the formation of magnetic anisotropy in the studied samples. Demagnetizing fields occurring on inhomogeneities of the surface relief can have a significant effect on the orientation of the axis of magnetic anisotropy in case of surface layers. This assumption requires additional experimental verification and the MIT method can also be used for the analysis of its results. It is also of interest to study the effect of the axial magnetic field on the radial distribution of the circular magnetic permeability in the studied wires using the MIT method.

Funding

This study was supported by grant from the Russian Science Foundation № 22-22-00709, <https://rscf.ru/project/22-22-00709/>.

Conflict of interest

The authors declare that they have no conflict of interest.

References

- [1] J. Liu, R. Malmhall, S.J. Savage, L. Arnberg. *J. Appl. Phys.*, **67**, 4238 (1990).
- [2] V. Madurga, A. Hernando. *J. Phys.: Condens. Matter*, **2**, 2127 (1990).
- [3] M. Vazquez, A. Hernando. *J. Phys. D: Appl. Phys.*, **29**, 939 (1996).
- [4] A.S. Antonov, V.T. Borisov, O.V. Borisov, V.A. Pozdnyakov, A.F. Prokoshin, N.A. Usov. *J. Phys. D: Appl. Phys.*, **32**, 1788 (1999).
- [5] K. Fodil, M. Denoual, C. Dolabdjian, A. Treizebre, V. Senez. *Appl. Phys. Lett.*, **108**, 173701 (2016). DOI:10.1063/1.4948286
- [6] J. Chen, J. Li, Y. Li, Y. Chen, L. Xu. *Sensors*, **18**, 732 (2018). DOI:10.3390/s18030732.
- [7] N.A. Usov, A.S. Antonov, A.N. Lagar'kov. *JMMM*, **185**, 159 (1998).
- [8] D.A. Bukreev, M.S. Derevyanko, A.A. Moiseev, A.V. Svalov, A.V. Semirov. *Sensors*, **22**, 9512 (2022). <https://doi.org/10.3390/s22239512>
- [9] A.V. Semirov, A.A. Moiseev, V.O. Kudryavtsev, D.A. Bukreev, N.P. Kovaleva, N.V. Vasyukhno. *ZhTF*, **85** (5), 137 (2015). (in Russian).
- [10] A.V. Semirov, V.O. Kudryavtsev, A.A. Gavrilyuk, A.A. Moiseev. *Pisma v ZhTF*, **32** (15), 137 (2006) (in Russian).
- [11] D.A. Bukreev, M.S. Derevyanko, A.A. Moiseev, A.V. Semirov, P.A. Savin, G.V. Kurlyandskaya. *Materials*, **13**, 3216 (2020). DOI:10.3390/ma13143216

Translated by A.Akhtyamov